RESEARCH ARTICLE OPEN ACCESS

Nontraditional Observations with the SMAP Radiometer

Ralph D. Lorenz*, Shannon M. Mackenzie**
**Johns Hopkins Applied Physics Laboratory, 11100 Johns Hopkins Road, Laurel, MD 20723, USA*
*** Johns Hopkins Applied Physics Laboratory, 11100 Johns Hopkins Road, Laurel, MD 20723, USA*
Corresponding Author : Ralph D. Lorenz

ABSTRACT
The SMAP (Soil Moisture Active Passive) satellite carries an exquisite microwave radiometer. This instrument, using a deployed 6m mesh antenna, makes polarimetric brightness temperature measurements at L-band (1.41 GHz) with a footprint of ~40km. While the mission is principally devoted to terrestrial hydrology and land use studies, we are exploring the use of this unique observatory for applications analogous to those that might exploit microwave radiometry at other planetary bodies, specifically towards the detection of volcanism on Venus and lightning on Jupiter or other bodies.
Keywords – Microwave Radiometry; Volcanism; Lightning; Radio Frequency Interference

---

Date Of Submission: 04-04-2019 Date Of Acceptance: 23-04-2019

I. INTRODUCTION

Microwave radiometers have a long history in planetary exploration – indeed, the very first instrument sent by NASA to another planet was the microwave radiometer on Mariner II, intended to resolve the question of how warm was the surface of Venus. Dedicated microwave radiometer instruments have also flown to a comet (MIRO on ESA's Rosetta), the Moon (the multi-band instrument on the Chinese Chang-E 1 lunar orbiter) and most recently the Multiwavelength Radiometer (MWR) at Jupiter on the JUNO mission. Additionally, a microwave radiometer capability can be frequently added with minimal cost to radar instruments (as in Magellan or Cassini) or even the spacecraft telecommunications system (as on the New Horizons mission), although these implementations may not enjoy as high precision as a dedicated instrument.

A microwave radiometer capability may be a useful means of detecting active volcanism [1] at Venus on a future radar mapping mission (recall that Magellan, nearly 30 years ago, mapped Venus only as well as Mariner 9 mapped Mars in ~1970). While most attention has focused on volcano monitoring in the near-infrared, this has the disadvantage of suffering from requiring essentially ongoing eruption beneath the spacecraft, since the dense atmosphere quickly quenches exposed lava surfaces to close to ambient. This is problematic for a mapping mission in a low circular orbit, in that Venus' slow rotation (sidereal day 243 Earth days) means that a given location will only be visible beneath a polar orbiter once every 121 days, and thus statistically an erupted lava will be 60 days old and unlikely to remain incandescent. Because microwave radiometry probes deeper into the planetary surface, it may pick up the heat within the lava flow, permitting detection months or years after eruption (e.g. [2]).

The disadvantage, of course, with microwave radiometry is that radio is on the wrong side of the Planck function, small regions of very hot temperatures only add a modest area-weighted brightness temperature increment, averaged over what is typically a rather large instrument footprint. This is in contrast to the near-infrared, where surfaces at a few hundreds of Kelvin radiate with spectral power densities many orders of magnitude above the background. Thus it would be desirable to assess volcanic detection by microwave radiometry at Earth before developing strong expectations at Venus. There have been speculative investigations of possible (nonthermal) microwave emissions associated with rock failures on volcanos [3,4], but (to these authors' knowledge) no investigation of microwave thermal emission changes at volcanoes.

A second application of microwave radiometry is in the study of lightning. Although radio emissions (typically at 10 kHz, but more generally from a few Hz to tens of kHz) are well-known from lightning discharges on Earth, there are only a handful of reports (e.g [5,6]) of emissions in the GHz range. Interest in this phenomenon has been stimulated, however, by the observation of lightning flashes at Jupiter by the JUNO MWR instrument [7]. While spaceborne detections of RF lightning emissions date back to the 70s, to date, there is no comparable satellite detection of terrestrial lightning at microwave wavelengths.

In this paper we describe some initial efforts to explore the SMAP radiometer capabilities

in these applications. Three volcanic events are considered, and some preliminary investigations into lightning are presented.

II. SMAP MICROWAVE RADIOMETER

The SMAP (Soil Moisture Active Passive) satellite was launched in 2015, with the objective of combining L-band (1.41 GHz) radiometry with higher-resolution Synthetic Aperture Radar (SAR) imagery at a similar wavelength, to derive a high-resolution soil moisture product for hydrology and land-use studies. It flies in a 690km sun-synchronous orbit, revisiting sites every 2-3 days.

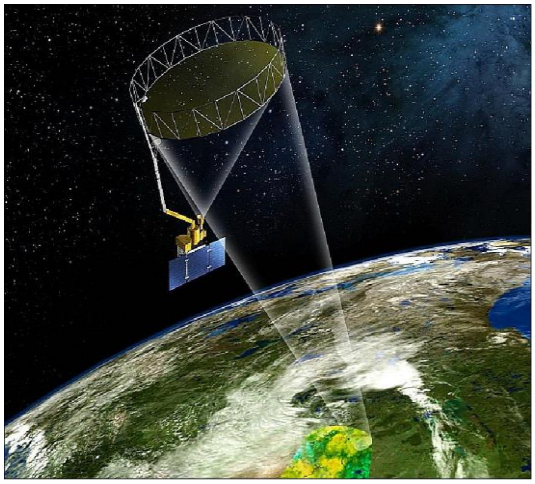

Figure 1. Artist's impression of the SMAP satellite in orbit. (NASA)

The instrument mechanically scans a 6m deployed mesh antenna reflector to sweep a radiometer beam with an instantaneous footprint of 39x47km in a ~1000km wide swath. The radiometer measures the brightness temperature T_b in V- and H-polarizations with an incidence angle of 40 degrees. The SAR system operated for several months before a low-voltage supply for the high-power amplifier failed. The radiometer continues to supply excellent data, however.

A significant challenge for microwave radiometry at Earth for geophysical applications, despite international treaties on electromagnetic spectrum allocations, is the large amount of anthropogenic radio noise [9]. These noise (Radio Frequency Interference – RFI) sources are widely dispersed and comprise emitters from air defense radars (notably the DEW stations in the arctic), to commercial radio systems (poorly-controlled cellphone signals, taxis and the like). RFI sources are for the most part geographically-static and can be partly screened out on this basis. RF emission, however, does not correlate as simply with economic activity as optical emission, it seems. For example, the Americas are overall relatively quiet, due to robust implementation of spectrum control.

Because RFI is such a significant challenge in Earth-orbiting radiometers, specific mitigation measures are included. On SMAP [8,10] these include kurtosis detection, as well as subsampling of the energy in each observation into 16 and 16 bins in time and frequency, respectively. RFI tends to be narrowband and/or pulsed, concentrating most of the energy into a small number of these bins.

For our applications in volcano detection, the RFI mitigations in general should not reject data of interest, since the energy is still thermal and thus noncoherent (not triggering kurtosis detection) and broad in frequency and time. Conceivably a strong local source could trigger an RFI flag as indicating an unexpected jump in T_b, but in this case the data will still be preserved.

For lightning detection, emission is quasi-impulsive, and thus it may be expected that RFI flags will be triggered (indeed, the noise on broadcast radio, especially older amplitude-modulated radio, is called 'static' because it is associated with electrical discharges.)

III. MAY 2018 KILAUEA ERUPTION

The 2018 eruption of Kilauea on Hawaii attracted significant media attention due to the destructive impact of lava flows on communities on the east part of the Big Island: the tourism industry also afforded the opportunity for graphic aerial observations (e.g. Figure 2). The progress of the eruption has been well-documented in-situ by the US Geological Survey, and via satellite infrared observations (figure 3) – see also [13].

Eruptions in the East Rift zone (distinct from the main volcano) began on May 3, 2018 and caused some $800M in property damage. By August 3, 35km^2 of terrain had been covered by lava flows, including about 3.5km^2 of new land where lava entered the ocean.

Figure 2. Rivers of lava in the 2018 Kilauea eruption. Note that the actual incandescent area is rather small (USGS).

This large and well-documented eruption seems superficially a strong candidate for detection

by microwave radiometry, in that the lava flows occupy a relatively large area (~2% of the SMAP footprint area). Note, however, that this area was emplaced over several months.

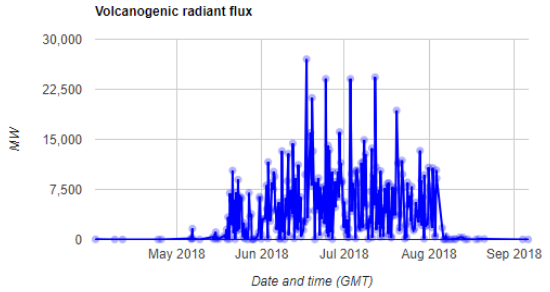

Figure 3. The history of the eruption as documented by the MODVOLC time series of satellite infrared observations (derived by U. Hawaii from Terra/Aqua MODIS data). The main phase of the eruption began in mid-May (circa Day of Year 130)

Laboratory measurements [11] of basalts, studied in some detail in support of Apollo, have microwave loss tangents δ of the order of 0.01-0.03, and the loss tangent of basalt lava flows on Mars has been estimated in-situ at 0.01-0.03 (at 20 MHz) using sounding radar [12].

With a loss tangent of 0.02 one would expect that SMAP (λ~20cm) might sense down to a depth of ~λ/δ of several meters, and indeed microwave radiometer measurements in cold Antarctic ice have been documented to penetrate to depths of several meters.

Calculations [1] show that if the eruption temperature is ~800K above ambient, and the lava cools conductively (with thermal diffusivity of $5x10^{-7}$ m^2/s), then the temperature excess of a cooling flow should still be >100K at depths of 0.2m even after a week (this ignores the buffering effect of latent heat, which will lead to even higher temperatures over time). Adopting a loss tangent of 0.02, the brightness temperature increment will be >350K after one day, and >200K after one week. After ~60 days (roughly the duration of the entire eruption), the Tb increment of the oldest parts of the flow will still be >40K, and crudely integrating the contributions of the oldest and youngest parts, a brightness temperature increment of the flows as a whole should be of the order of 100K.

This perturbation over the 35 km^2 Hawaii flows is diluted by a factor of ~50 by the relatively large SMAP footprint (~2000 km^2) and so the observable footprint-averaged ΔT_b~ 2K. This is in principle (just) within the radiometric resolution of the SMAP instrument.

Unfortunately, the problem is one of detecting this signal against a rather fluctuating background, and in fact over this part of Hawaii the background has a rather severe variation (figure 4) – in fact of the order of 100K.

This situation results largely from the proximity of the coastline (only ~3km from the vent system), where a strong dielectric contrast exists between the land (T_b~230K) and the ocean (T_b~100K). Thus, the observed T_b depends rather critically on the fraction of the footprint occupied by ocean and thus the exact footprint location. Selecting only those footprints centered close to the vent improves matters somewhat, but signals of ΔT_b<~10K would still be difficult to detect and thus we cannot as yet claim to see a signature of the eruption.

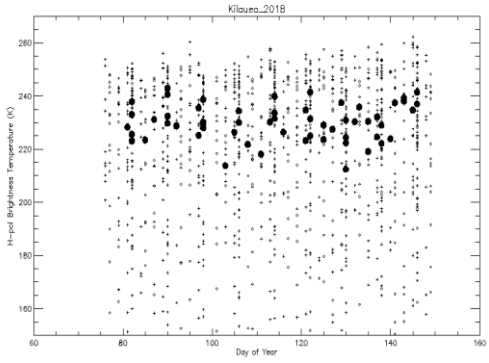

Figure 4. SMAP H-pol brightness temperatures from the L1B data product, on a ~70 day period centered about the start of the eruption. Small crosses include all footprints containing the east rift eruption site, and have a very wide scatter owing to the varying fraction of ocean present. The solid circles are only those footprints centered within ~5 km of the site – although their scatter is much less, it is still rather large.

IV. JANUARY 2017 ERTA ALE ERUPTION

To avoid the challenge of the strong land/sea brightness temperature contrast adjacent to the eruption, we have examined an inland basaltic eruption, the 2017 activity at Erta Ale in Ethiopia.

This volcano features a historically-continuous lava lake at its summit. In 2017, a major lava exposure emerged further to the south, and flows progressively extended east and west (Figure 5).

After the initial spike of 4.5GW, the steady infrared radiated power (figure 6) rose to a plateau of about 1.5 GW in April 2017 and then declined over the next year to about a third of that value. Note that the infrared record is 'spiky' since the observed flux can be reduced by cloud cover or (in the case of lava deep in pits or cracks, by terrain obstruction).

The scatter in T_b is gratifyingly lower (Figure 7) than for Hawaii, due perhaps to lower variability in surface moisture associated with rain (Erta Ale is in the Afar Depression, one of the

hottest, driest places on Earth!) as well the fact that the site is ~110km away from the Red Sea so the ocean/land contrast issue is not a factor here.

Figure 5. Landsat near-infrared image, (USGS, processed by ESA/Copernicus.) Annotations by Culture Volcan via Smithsonian Global Volcanism Program. The semipermanent summit lava lake is visible at upper left: the new lava lake is at its 5 o'clock, and the incandescent fronts of the new lava flows are at 2- and 7-o'clock from there, extending 5 and 3.5km respectively. The total area of new lava may be estimated as of the order of ~10km^2.

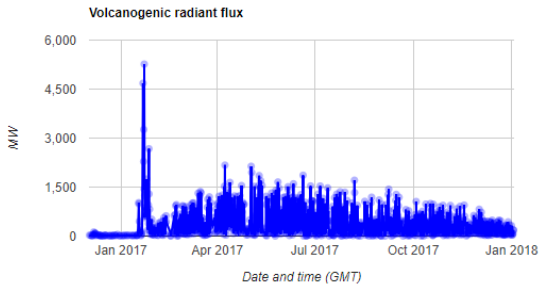

Figure 6. Erta Ale MODVOLC time series. After the initial spike a broad peak in near-IR emission builds and decays.

Inspection of the SMAP T_b data for early 2017 (Figure 7) does not show an obvious jump in January – however, it may be that that initial spike was associated with a small but very hot emission: a 1 km^2 lava flow at 1000 K above ambient gives only a 0.5K ΔT_b over the radiometer footprint. The slow buildup of lava flow area, while overall yielding a higher footprint-averaged ΔT_b, is a difficult signal to discriminate against e.g. seasonal temperature changes.

The data do show, at least, that the background fluctuations in this inland desert region are much lower than for Hawaii – in this sequence the variations are only of the order of 5K. In further work we will explore whether differential measurements (e.g. T_b at the target location minus T_b at a nearby location) offer superior detection characteristics.

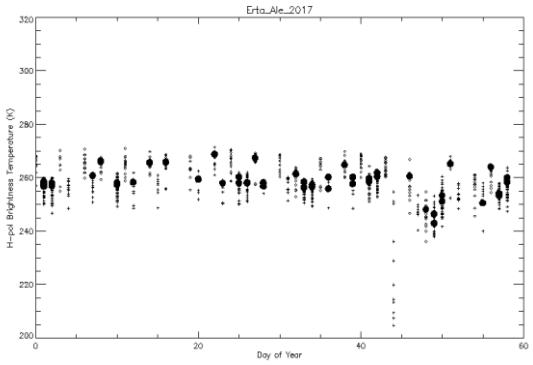

Figure 7. SMAP H-Pol brightness temperatures in early 2017 – here the scatter is much lower (~10K), and is not substantially improved by tighter location selection (black circles). The drop at DOY 48 is significant, and may be associated with rainfall.

V. FUEGO GUATEMALA

Unlike basaltic volcanos like Kilauea and Erta Ale which principally deposit lava flows locally, more silicic volcanoes may erupt ash which can be deposited over much wider areas. The local temperature perturbation may be much lower, of course, but the larger area may make such eruptions more amenable to yielding signatures in microwave radiometry. For example, the 2010 Ejyafjallajökull eruption in Iceland (sadly prior to the SMAP epoch) deposited ash over an area several times larger than the SMAP footprint.

A prominent eruption of this style during the SMAP operation period is Fuego in Guatemala, a 3760m-high stratovolcano. On 3 June 2018, this volcano (continuously active at some level at least since the Spanish conquest), erupted violently [13], burying several towns in pyroclastic density flows and lahars (mud flows), leading to over 150 confirmed deaths, although some thousands may have been killed. Ash deposits prompted the closure of La Aurora international airport in Guatemala city, ~40km away.

One might expect a dry ashfall deposit to have two signatures in microwave radiometry, both leading to increased T_b. First, a sufficiently deep and hot deposit (such as the deposits near Mt St Helens – where temperatures of >300°C were retained in 2-3m thick layers ~3 weeks after the eruption [14]) will provide a strong thermal signature in the same way a lava flow might. This signature will only slowly decay by conduction (unless or until rainfall quenches the heat and/or compacts the ash) – e.g. the Mt. St. Helens ash was still at 100°C 86 days after emplacement. Second, even a deposit of a few cm, which if emplaced warm will cool quickly anyway, has a dielectric rather than thermal signature. Crudely, much like the dry sands

which permit SAR imaging to detect buried river channels (e.g. [15]), the low-density ash deposit serves as an impedance-matching layer (much like the anti-reflective coatings on optical lenses) which will increase the emissivity of a high-density substrate.

Although the volcano is 65km from the sea, our efforts to detect a signature have been substantially thwarted by the heavy RFI in this area, such that there are actually very few valid footprints. We await further large eruptions of this sort in RF-quiet locations.

VI. DISCUSSION – VOLCANO DETECTION

The Erta Ale data suggest that in desert regions at least, a natural variability in the footprint-averaged brightness temperature of ~5 K is typical. Thus, to be 'obvious', a ~5K increase in brightness temperature may be required: this corresponds to an area-temperature increment of ~10,000 K-km^2 associated with the volcanic deposit. This appears to be close to what one might expect from the 2018 Hawaii eruption, but a factor of a few larger than the Erta Ale eruption.

More elaborate detection schemes are possible than the simple examination of variance and mean of the T_b time series, in that there is strong prior information. First, the brightness temperature variation should be approximately a step change – a hot lava flow is relatively suddenly emplaced, and cools (at the depth sounded by instrument) at a relatively slow rate. Second, strong prior information on the site of an eruption exists, since the volcano location is known (this is also true for Venus). Third, for lava flows at least, it can be assumed that the source is rather small compared with the footprint: an extensive body of work exists in the radio astronomy community on the detection and location of point sources in low-resolution data. In the terrestrial application, other data (e.g. seismic, field observations, satellite thermal infrared etc.) also constrain the time, location and extent of an eruption. These priors allow more sensitive detection tests to be applied. Additionally, differential measures (e.g. using nearby reference points to decorrelate regional changes in Tb from weather-related effects) may offer higher sensitivity.

It may be that using a single (ambient temperature) value for the loss tangent is overly optimistic, in that loss tangents for many materials tend to increase toward the melting point. This phenomenon is in fact instrumental in a 'thermal runaway' effect encountered in microwave thermal processing of basalt. Hence a hot lava flow being interrogated by radiometry will in fact become progressively more opaque near the melting level, such that fully molten temperatures may in fact never be observed even if the flow is molten at depth.

Another possibility is that many volcanic eruptions are attended by sufficient precipitation (either by virtue of steam erupted with the lava causing local cloud and rain, or by virtue of being in tropical areas with frequent rainfall like Hawaii, or both) that the lava flow is cooled to depth much more rapidly than conductive cooling would suggest. Aqueous alteration of the basalt, and the retention e.g. of thin surface films of water (especially if rendered conductive by dissolved sulfuric acid) could substantially increase the loss tangent above that of dry (e.g. Martian or lunar) rock.

Unless these confounding effects are common and/or significant, consideration of the volcanic record suggests that sooner or later an eruption with 'obvious' detectability should occur. In the meantime, we will explore more sensitive detection measures.

VII. LIGHTNING

There has been extensive study of storm systems on Earth with microwave methods (notably weather radar can probe the structure of a cloud that is obscured from optical interrogation). However, only a few reports of microwave 'flash' detection of lightning exist – the RF emission from lightning discharges has a relatively steep red spectrum, with emission falling off as f^{-2} or some similar power. Nonetheless, impulsive signals recorded in the 0.6 GHz radiometer of the Juno spacecraft [7] have proven recently to be an effective means of mapping out lightning discharges on Jupiter.

As an initial reconnaissance study, we explored a region in East Africa which is known (from long-distance VLF triangulation in the World Wide Lightning Location Network WWLLN, and from satellite optical observations [16]) to be a 'hotspot' [17] for lightning flashes. This area appears to have enhanced activity as winds blow moist air from Lake Kivu up into nearby highlands. This lifting triggers strong convection in the moist tropical atmosphere and frequent lightning.

We did indeed find many RFI trigger flags in data in this region, but close examination (Figure 8) shows that they are concentrated not quite in the area of high lightning activity, but instead at three major cities in the area.

It is not immediately obvious why these cities (populations 0.25 to 1 million) should have RFI but other similar-sized cities like Bujumbura do not; all have airports for example. It may be that there are military installations involved, or merely a different regulatory regime e.g. on TV broadcasting. It may well be that there are interesting socioeconomic studies to be pursued on RFI characteristics, in an analogous manner to the use of

night-time luminosity data as a proxy of gross domestic product [18].

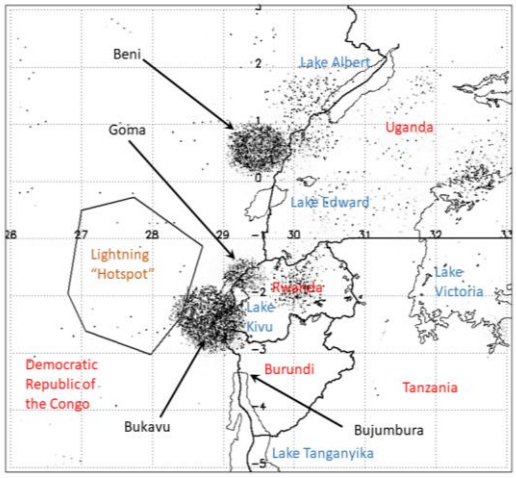

Figure 8: Survey of anomalous SMAP brightness temperatures in East Africa. Dots show locations where RFI flags were triggered and the antenna temperature in a given footprint was 5K or more above the previous footprint, in swaths for the period January 1, 2018 to April 28, 2018. There is no particular concentration of events in the lightning hotspot known from other studies, nor in some cities (e.g. Bujumbura). Strong concentrations of RFI events appear around the cities of Bukavi, Goma and Beni.

Returning to lightning, our most promising strategy will likely then be to examine locations where specific storms have occurred during SMAP overflights, of areas where RFI has a low prior probability (e.g. over the oceans). The recent commissioning of the Geostationary Lightning Mapper (GLM) instrument on the GOES satellite may be of particular use in this respect.

VIII. CONCLUSIONS

The goal of this effort, to detect microwave emission signatures of volcanic activity, has not yet been achieved. The challenges in detection on Earth appear principally to be fluctuating background associated with weather (and moisture especially), the presence of strong dielectric boundaries (ocean shoreline) and the presence of RFI. Volcanic signatures may yet be detected in SMAP data if a sufficiently large eruption occurs at a location where these confounding effects are modest: in favorable locations (e.g. Erta Ale), area-temperature perturbations of the order of 10,000 K-km^2 should be readily detectable, but more sensitive detection schemes may yield better sensitivity.

We have noted the possibility of detecting lightning flashes with SMAP, and efforts to make such detections are underway. Finally, we also note the potential for socioeconomic studies exploiting SMAP data.

ACKNOWLEDGEMENTS

This work is supported by NASA via the Scientific Utilization of SMAP (SUSMAP) program Grant NNX16AN36G. We acknowledge useful discussions with Jeff Piepmeier, Priscilla Mohammed and colleagues at GSFC on the radiometer instrument and its RFI handling. Our project has benefited from the University of Hawaii MODVOLC and Turin/Florence MIROVA volcano surveillance products using MODIS data. MIROVA (Middle InfraRed Observation of Volcanic Activity), a collaborative project between the Universities of Turin and Florence (Italy) supported by the Centre for Volcanic Risk of the Italian Civil Protection Department (URL: http://www.mirovaweb.it/). European Space Agency (ESA), Copernicus.

REFERENCES

[1]. Lorenz, R.D., Le Gall, A. and Janssen, M.A., 2016. Detecting volcanism on Titan and Venus with microwave radiometry. Icarus, 270, pp.30-36..

[2]. Bondarenko, N.V., Head, J.W. and Ivanov, M.A., 2010. Present- day volcanism on Venus: evidence from microwave radiometry. Geophysical Research Letters, 37(23). https://doi.org/10.1029/2010GL045233

[3]. Maeda, T. and Takano, T., 2008. Discrimination of local and faint changes from satellite-borne microwave-radiometer data. IEEE Transactions on Geoscience and Remote Sensing, 46(9), pp.2684-2691.

[4]. Takano, T., Maeda, T., Miki, Y., Akatsuka, S., Hattori, K., Nishihashi, M., Kaida, D. and Hirano, T., 2013. Detection of microwave emission due to rock fracture as a new tool for geophysics: A field test at a volcano in Miyake Island, Japan. Journal of Applied Geophysics, 94, pp.1-14.

[5]. Kosarev, E.L., Zatsepin, V.G., Mitrofanov, A.V., 1970. Ultrahigh frequency radiations from lightning. J. Geophys. Res. 75 (36), 7524–7530.

[6]. Petersen, D. and Beasley, W., 2014. Microwave radio emissions of negative cloud-to-ground lightning flashes. Atmospheric research, 135, pp.314-321.

[7]. Brown, S., Janssen, M., Adumitroaie, V., Atreya, S., Bolton, S., Gulkis, S., Ingersoll, A., Levin, S., Li, C., Li, L. and Lunine, J., 2018. Prevalent lightning sferics at 600 megahertz near Jupiter's poles. Nature, 558(7708), p.87.

[8]. Piepmeier, J.R., Focardi, P., Horgan, K.A., Knuble, J., Ehsan, N., Lucey, J., Brambora, C., Brown, P.R., Hoffman, P.J., French, R.T. and Mikhaylov, R.L., 2017. SMAP L-band microwave radiometer: Instrument design and first year on orbit. IEEE Transactions on Geoscience and Remote Sensing, 55(4), pp.1954-1966.

[9]. Njoku, E.G., Ashcroft, P., Chan, T.K. and Li, L., 2005. Global survey and statistics of radio-frequency interference in AMSR-E land

observations. IEEE Transactions on Geoscience and Remote Sensing, 43(5), pp.938-947.
[10]. Mohammed, P.N., Aksoy, M., Piepmeier, J.R., Johnson, J.T. and Bringer, A., 2016. SMAP L-band microwave radiometer: RFI mitigation prelaunch analysis and first year on-orbit observations. IEEE Transactions on Geoscience and Remote Sensing, 54(10), pp.6035-6047.
[11]. Campbell, M.J. and Ulrichs, J., 1969. Electrical properties of rocks and their significance for lunar radar observations. Journal of Geophysical Research, 74(25), pp.5867-5881.
[12]. Carter, L.M., Campbell, B.A., Holt, J.W., Phillips, R.J., Putzig, N.E., Mattei, S., Seu, R., Okubo, C.H. and Egan, A.F., 2009. Dielectric properties of lava flows west of Ascraeus Mons, Mars. Geophysical Research Letters, 36(23) doi: 10.1029/2009GL041234
[13]. Smithsonian Volcano Observatory Bulletin http://volcano.si.edu/
[14]. Keating, G.N., 2005. The role of water in cooling ignimbrites. Journal of Volcanology and Geothermal Research, 142(1-2), pp.145-171.
[15]. Elachi, C., Roth, L.E. and Schaber, G.G., 1984. Spaceborne radar subsurface imaging in hyperarid regions. IEEE Transactions on Geoscience and Remote Sensing, (4), pp.383-388.
[16]. Soula, S., Kasereka, J.K., Georgis, J.F. and Barthe, C., 2016. Lightning climatology in the Congo Basin. Atmospheric Research, 178, pp.304-319.
[17]. Albrecht, R.I., Goodman, S.J., Buechler, D.E., Blakeslee, R.J. and Christian, H.J., 2016. Where are the lightning hotspots on Earth?. Bulletin of the American Meteorological Society, 97(11), pp.2051-2068.
[18]. Chen, X. and Nordhaus, W.D., 2011. Using luminosity data as a proxy for economic statistics. Proceedings of the National Academy of Sciences, 108(21), pp.8589-8594.